## PAPER

Check for updates

# Assessing the compatibility of primary human hepatocyte culture within porous silk sponges†

David A. Kukla,[a] Whitney L. Stoppel, (ID) ‡[b] David L. Kaplan (ID) [b] and Salman R. Khetani (ID) *[a]

Donor organ shortages have prompted the development of alternative implantable human liver tissues for patients suffering from end-stage liver failure. Purified silk proteins provide desirable features for generating implantable tissues, including sustainable sourcing from insects/arachnids, biocompatibility, tunable mechanical properties and degradation rates, and low immunogenicity upon implantation. While different cell types were previously cultured for weeks within silk-based scaffolds, it remains unclear whether such scaffolds can be used to culture primary human hepatocytes (PHH) isolated from livers. Therefore, here we assessed the compatibility of PHH culture within porous silk scaffolds that enable diffusion of oxygen/nutrients through the pores. We found that incorporation of type I collagen during the fabrication and/or autoclaving of porous silk scaffolds, as opposed to simple adsorption of collagen onto pre-fabricated silk scaffolds, was necessary to enable robust PHH attachment/function. Scaffolds with small pores ($73 \pm 25$ µm) promoted larger PHH spheroids and consequently higher PHH functions than large pores ($235 \pm 84$ µm) for at least 1 month in culture. Further incorporation of supportive fibroblasts into scaffolds enhanced PHH functions up to 5-fold relative to scaffolds with PHHs alone and 2D co-cultures on plastic. Lastly, encapsulating PHHs within protein hydrogels while housed in the silk scaffold led to higher functions than protein hydrogel-only or silk-only controls. In conclusion, porous silk scaffolds containing extracellular matrix proteins can be used for the culture of PHHs ± supportive non-parenchymal cells, which can be further built on in the future to create optimized silk-based liver tissue surrogates for cell-based therapy.

## Introduction

Liver functions can be severely compromised by several diseases. In particular, drug-induced liver injury is the leading cause of drug attrition,[1] while hepatitis B and C viruses chronically infect ∼400 million and ∼170 million people, respectively, and can lead to fibrosis, cirrhosis, and hepatocellular carcinoma (HCC), the third leading cause of deaths from cancer globally.[2] Additionally, non-alcoholic fatty liver disease is on an epidemic rise and can also lead to fibrosis, cirrhosis, and HCC.[2] Overall, chronic liver disease affects >500 million people, causing 2% of all deaths globally.[3,4] Currently, orthotopic liver transplantation is the only treatment for liver failure shown to directly alter mortality.[5] However, there is a severe shortage of viable donor livers to satisfy increasing demand; for example, 8250 liver transplants were performed in the US in 2018 whereas there are almost 14 000 patients currently on the waiting list (American Liver Foundation). Therefore, there is an urgent need for alternative cell-based therapies that can serve as a bridge to liver transplantation and eventually as a complete organ replacement.

Given significant species-specific differences in liver functions, human liver cells are utilized for fabricating platforms for cell-based therapies as well as drug development.[6] However, immortalized cell lines display abnormal growth and low liver functions,[7] while protocols to generate autogenic induced pluripotent stem cell-derived hepatocyte-like cells require further improvements to enable adult-like functions.[8] Therefore, primary human hepatocytes (PHHs), that perform the majority of functions in the liver *in vivo*, are considered ideal for building human liver platforms. While freshly isolated PHHs are in limited supply, efforts are underway to harness the tremendous *in vivo*-like growth potential of PHHs using small molecules and/or growth factors *in vitro*;[9] additionally, PHHs can be expanded *in vivo* in rodents by stimulating the rodent to produce regenerative factors,[10] though there remain concerns over zoonotic transfer.

Others have previously fabricated 3-dimensional (3D) implantable liver constructs containing PHHs housed within

[a]Department of Bioengineering, University of Illinois at Chicago, 851 S Morgan St, 218 SEO, Chicago, IL 60607, USA. E-mail: skhetani@uic.edu; Fax: +1-312-996-5921; Tel: +1-312-413-9424

[b]Department of Biomedical Engineering, Tufts University, Medford, MA, USA

different biomaterials specifically designed for cell-based therapies as opposed to *in vitro* drug screening. Some popular biomaterials have been naturally-derived alginate and chitosan as well as synthetic polyethylene glycol diacrylate (PEGDA) and poly(lactic acid) (PLA) modified with cell adhesive peptide (*e.g.* RGDS) to enable cell attachment. While PHHs encapsulated into alginate microbeads functioned for 3 days *in vitro* and improved liver functions in rodents with acute liver failure for ∼7 days,[11] it is not clear if alginate microbeads without further chemical modification can be used to support PHH culture for >1 week. Chen *et al.* encapsulated PHHs and supportive fibroblasts within PEGDA–RGDS hydrogels *via* UV crosslinking and demonstrated liver functions for 8 days *in vitro*; furthermore, intraperitoneal implantation of these constructs into rodent models showed penetration of host vasculature and liver function for 2 weeks *in vivo*.[12] However, the use of UV cross-linking to encapsulate cells into PEGDA may induce long-term genotoxicity and/or other signaling changes in PHHs. Additionally, besides being mechanically weak, PEGDA requires modification with protease-activated peptides to render it biodegradable for integration with host tissue, which adds to fabrication complexity and cost, in addition to other immune response issues to the degrading PEGDA gel that has prompted others to develop alternative culture platforms to address some of these issues.[13,14] While both chitosan modified with galactosylated hyaluronic acid[15] and PLA[16] modified with extracellular matrix (ECM) proteins have been used for hepatocyte culture for 5–15 days *in vitro*, these studies have been restricted to either rat hepatocytes or cancerous hepatic cell lines, which do not fully represent PHH functions and often require different culture conditions than their PHH counterparts.[6,7] Furthermore, chitosan scaffolds typically have low mechanical stability and a lack of porosity tunability,[17] while PLA induces a more severe inflammatory reaction in animal models than collagen or silk films.[18] Therefore, there is a need to further explore alternative biomaterials useful for fabricating optimal cell-based therapies containing biodegradable degradation products, which do not elicit a negative immune response.

Scaffolds made of silk fibroin protein are known to be biocompatible both in their native state and in terms of their enzymatic degradation products. Silk fibroin-based biomaterials have been shown to support long-term (months) culture of cells *in vitro* without initiating unwanted cell-specific signaling.[19–21] Formation of these scaffolds occurs without the need for chemical or UV-based crosslinking and the structure is maintained both under perfusion in a bioreactor or in a well plate with cell culture medium.[22,23] Additionally, silk scaffolds can be autoclaved for contaminant-free culture.[24–26] From a manufacturing perspective, silk scaffolds can be (a) fabricated using proteins secreted by many insect/arachnid species (*e.g.* silkworms and spiders), (b) molded into a wide range of forms (*e.g.* hydrogels and sponges), (c) tuned for porosity while maintaining robust bulk mechanical properties and *in vivo* degradation rates,[24,26] and (d) combined with other materials (*e.g.* ceramics and extracellular matrix or ECM proteins) to create composites that modulate cell responses.[24,27] When implanted *in vivo*, silk sponges and other formats can induce

a transient (weeks) mild and beneficial inflammatory response that induces vascular ingrowth but does not activate the adaptive immune response nor the formation of a permanent fibrotic capsule.[23] Furthermore, silk scaffold degradation into non-toxic byproducts *in vivo* can be extended for months to allow native tissue remodeling.[28]

Silk scaffolds have been previously used for hepatocyte culture with positive functional and implantation outcomes. Specifically, primary rat hepatocytes seeded onto silk/chitosan scaffolds showed reduced inflammatory response relative to synthetic scaffolds;[29] rat hepatocytes seeded onto silk/RGD scaffolds demonstrated improved gene expression for 3+ weeks over 2D culture;[30] co-cultures of rat hepatocytes and stellate cells in silk scaffolds demonstrated improved functions for 2 weeks than hepatocyte monocultures.[31] In human-relevant studies, the QZG human hepatic cells seeded onto silk/gelatin scaffolds demonstrated infiltration of host cells after implantation into a rodent model,[32] and cancerous HepG2 cells seeded onto silk/RGD scaffolds demonstrated improved gene expression over 2D culture.[30] While the studies above are promising for the use of silk/protein scaffolds for hepatocyte culture *in vitro* and implantation *in vivo* in animal models, the application of such scaffolds for long-term (1+ month) PHH cultures ± supportive non-parenchymal cells (NPC) has yet to be realized. Therefore, here we sought to determine the functional behavior of PHHs within porous silk sponges (scaffolds) incubated with type I collagen during different steps of scaffold processing. Next, we examined how the inclusion of NPCs affects PHH functions in silk/collagen scaffolds over weeks and then months in culture. Finally, we encapsulated PHH/NPC co-cultures within ECM gels and determined whether ECM gel fidelity and PHH functions in the gel were modulated when placed within the porous silk scaffolds.

## Methods

### Preparation of porous silk sponges (scaffolds)

Silk fibroin solution was prepared as previously reported.[23,24,33] Briefly, pure silk fibroin was extracted from *Bombyx mori* cocoons by degumming 5 grams of fibers in sodium carbonate solution (0.02 M) to remove sericin. Degummed fibroin fibers were rinsed in distilled water and solubilized in aqueous lithium bromide (9.3 M) for 4 hours at 60 °C. The solution was dialyzed against deionized water until the conductivity of the dialysis water was <10 μS cm$^{-1}$. The solubilized silk solution was centrifuged to remove insoluble particulates. The final concentration was 3% wt/v silk solution. To fabricate collagen incorporated silk, 1 mg mL$^{-1}$ rat tail collagen I (Corning Life Sciences, Tewksbury, MA) in distilled water was added to a 3% wt/v silk fibroin solution. Aqueous silk solutions ± incorporated collagen were dispensed into wells of a 6-well plate. Silk ± incorporated collagen was frozen overnight at −20 °C and lyophilized at either −20 °C or −80 °C to create a network of thin, sheet-like lamellae with interconnected pores with either large (∼235 μm ± standard deviation of 84 μm) or small (∼73 μm ± standard deviation of 25 μm) pores, respectively. Dry scaffolds were removed and rendered insoluble by autoclaving
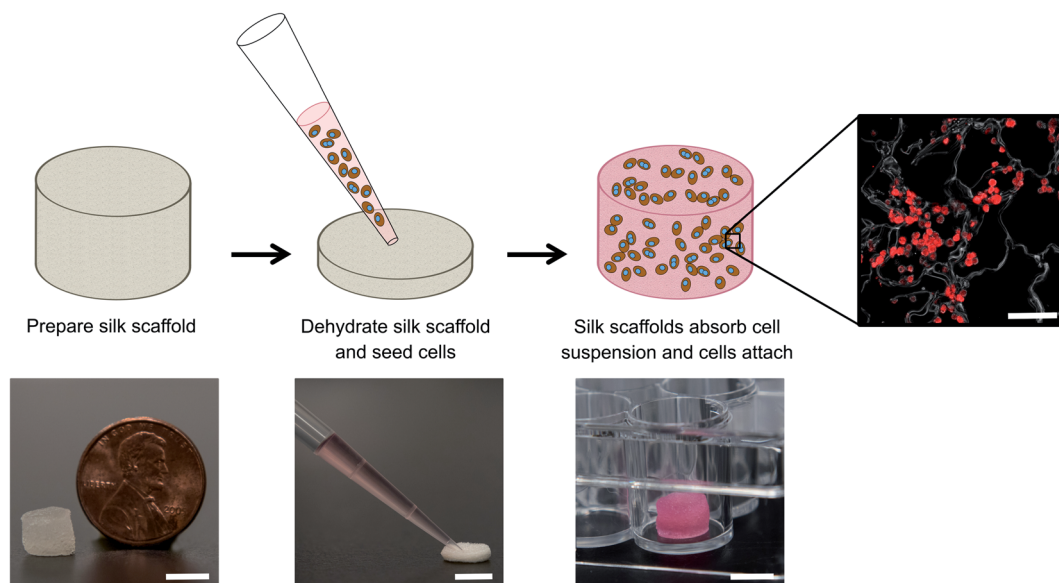
Fig. 1 Culture of cells within porous silk sponges (scaffolds). Left to right: Insoluble silk scaffolds containing type I collagen (from rat tails) were fabricated and autoclaved per the protocols described in methods and then partially dehydrated by manually squeezing the hepatocyte culture medium out of the pores. The scaffolds were subsequently placed within the wells of a 48-well plate which was pre-coated with Pluronic F-127 to prevent cell attachment to the plastic. A cell suspension of PHHs ± 3T3-J2 fibroblasts was seeded onto the partially dehydrated silk scaffolds, which wicked up the cell suspension and allowed cells to attach over 3–4 hours at 37 °C to the collagen within the silk scaffolds. Once cells attached, additional cell culture medium was added to the wells and replaced every 4 days with fresh medium. Culture medium was collected for supernatant-based assays and the cell-laden scaffolds were also fixed at specific time-points for immunostaining of hepatic markers. PHHs stained with a human albumin antibody are shown to the right. Top row scale bar is 100 μm and bottom row scale bars are 5 mm.

at 121 °C for 20 minutes at 15 psi in either 1× phosphate-buffered saline (PBS) or 1 mg mL$^{-1}$ collagen in 1× PBS to induce β-sheet formation, forming scaffolds that have previously been shown to display Young's moduli of ∼150–300 kPa and ultimate tensile strength of ∼60–100 kPa.[24] Scaffolds were cut to size using 6 mm biopsy punches ($h \times w$: 4.4 ± 0.3 mm × 5.7 ± 0.3 mm) and stored in 1× PBS at 4 °C until use for cell culture. Silk scaffolds without any collagen incorporation *via* the processing steps above (*i.e.* scaffolds autoclaved in 1× PBS alone) were placed in 1 mg mL$^{-1}$ collagen in 1× PBS for 2 hours at 37 °C to enable passive collagen adsorption.

## Cell culture

Cryopreserved PHHs were purchased from vendors permitted to sell products derived from human organs procured in the United States of America by federally designated Organ Procurement Organizations (BioIVT, Baltimore, MD, and Lonza, Walkersville, MD). PHH lots included HUM4055A (54 year-old female Caucasian) from Lonza and EJW (29 year old female Caucasian) from BioIVT. PHHs were thawed, counted, and viability was assessed as previously described.[34] 3T3-J2 murine embryonic fibroblasts were passaged as previously described and for some experiments, growth arrested by incubating in culture medium containing 1 μg mL$^{-1}$ mitomycin-C (Sigma-Aldrich) for 4 hours before trypsinization.

Before cell seeding, 48-well culture plates were coated with 5% w/v Pluronic™ F-127 (Sigma-Aldrich, St. Louis, MO) to make the surface of the tissue culture plastic non-adherent to cells.[35] Furthermore, all types of porous silk scaffolds described above

were placed in hepatocyte culture medium containing 10% fetal bovine serum (FBS, Thermo Fisher, Waltham, MA) overnight to promote protein binding to the silk surface before cell seeding. Other components of the hepatocyte culture medium were described previously.[34]

Cell suspensions were prepared in culture medium containing either PHH only (4 × 10$^6$ cells per mL), co-cultures of PHHs and growth-competent 3T3-J2 fibroblasts, or co-cultures of PHHs with growth-arrested 3T3-J2 fibroblasts; the ratio between the two cell types was kept at 1 : 1 (8 × 10$^6$ total cells per mL). For certain conditions, cells were suspended in either 4 mg mL$^{-1}$ rat tail collagen I or growth factor reduced Matrigel™ (Corning Life Sciences) solutions. Silk scaffolds were partially dehydrated by manually squeezing the hepatocyte culture medium out and then the scaffolds were placed within the Pluronic F-127-coated wells of the 48-well plate. The above-mentioned cell suspensions were seeded onto the partially dehydrated silk scaffolds at 125 μL per scaffold (500k PHHs ± 500k 3T3-J2 fibroblasts); the dehydrated silk scaffolds rapidly absorbed the cell suspensions (Fig. 1). Cells were then allowed to attach to the scaffold for ∼3–4 hours at 37 °C; cell suspension that pooled to the bottom of the well was periodically pipetted back onto the scaffolds during this timeframe to promote further cell attachment to the scaffold. After cell attachment, additional culture media (500 μL per well) was added to each well. For control conditions, cell suspensions in the collagen or Matrigel solutions were pipetted directly into the wells and allowed to polymerize as hydrogels in the absence of silk at 37 °C. All cultures were maintained *in vitro* for up to ∼5 months with culture medium changes every 4 days.
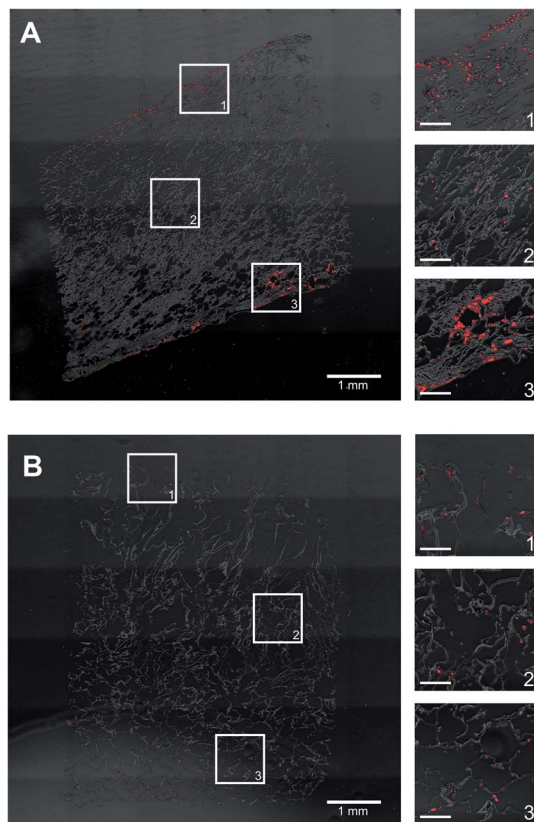
**Fig. 2** PHH distribution within composite silk–collagen I scaffolds of small or large pore sizes. Silk scaffolds containing collagen I were fabricated with (A) small pores (73 ± 25 μm) or (B) large pores (235 ± 84 μm) and then PHHs were seeded into the scaffolds per the protocols described in methods. After 3 weeks, the cell-laden scaffolds were fixed, sectioned, and stained for intracellular albumin. Shown in both panels is a single section and magnified images from three different regions within the scaffold to show the distribution of PHH attachment. The scale bars in magnified images are 250 μm.

## Hepatocyte functional assessments

Culture supernatants were assayed for albumin using a sandwich enzyme-linked immunosorbent assay (ELISA) kit with horseradish peroxidase detection (Bethyl Laboratories, Montgomery, TX) and 3,3′,5,5′-tetramethylbenzidine (TMB, Rockland Immunochemicals, Boyertown, PA) as the substrate. Absorbance values were quantified on the Synergy H1 multi-mode plate reader (BioTek, Winooski, VT). Cytochrome P450 2A6 (CYP2A6) enzyme activity was measured by incubating the cultures with 50 μM coumarin (Sigma-Aldrich) for 3 hours. The metabolite, 7-hydroxycoumarin (7-HC, Sigma-Aldrich), generated from coumarin was quantified *via* fluorescence detection (excitation/emission: 355/460 nm) using a standard curve on the Synergy H1 multi-mode plate reader.

## Cell staining

Scaffolds were fixed in 10% formalin solution (Sigma-Aldrich) overnight at 4 °C and rinsed with 1× PBS. Fixed samples were embedded in paraffin following a series of xylene and graded ethanol incubations and cut into 8 μm thickness vertical cross-

sections. Before cell staining, sections were deparaffinized. The fixed cultures were permeabilized and blocked using 0.3% Triton X-100 (Amresco) with 1% bovine serum albumin (BSA, Fisher Scientific) in 1× PBS for 4 hours at room temperature. Rabbit anti-human albumin (1 : 100) (Rockland Immunochemicals) or mouse anti-human CYP3A4 (1 : 100) (GeneTex, Irvine, CA) antibodies were added with 0.3% Triton X-100 and 0.1% BSA in 1× PBS (dilution solution) and incubated overnight at 4 °C. Cultures were then washed three times with 1× PBS. Cultures were labeled with either goat anti-rabbit IgG (H + L) Alexa Fluor 555 antibody (1 : 100) (Thermo Fisher Scientific) or rabbit anti-mouse FITC antibody (1 : 100) (GeneTex) in dilution solution for 3 hours at room temperature. After three 1× PBS washes, cultures were imaged using an Olympus IX83 microscope (Olympus America, Center Valley, PA).

## Data analysis

All findings were confirmed in 2–3 independent experiments (3–4 wells per condition and experiment). Data processing was performed using Microsoft Excel. GraphPad Prism (La Jolla, CA) was used for displaying results. Mean and standard deviation are displayed for all data sets. Statistical significance was determined using Student's *t*-test or one-way ANOVA followed by a Bonferroni pair-wise *post hoc* test ($p < 0.05$).

## Ethics approval

Ethics approval is not required for this study and this study is exempt from IRB approval; de-identified cryopreserved primary human hepatocytes were purchased from vendors permitted to sell products derived from human organs procured in the United States of America by federally designated Organ Procurement Organizations.

# Results

## Porous silk/collagen scaffolds can support PHH functions for at least 1 month in culture

PHHs are an adherent cell type that requires ECM proteins for optimal function; type I collagen extracted from rat tails (herein referred to as collagen I) is a popular ECM protein choice for PHH culture due to its abundant and cost-effective availability. Therefore, here we determined the optimal process of incorporating collagen I into our porous silk scaffolds. Porous silk scaffolds were initially prepared as described in methods, where silk fibroin solutions were frozen at −20 °C, lyophilized at either −20 °C or −80 °C, and rendered insoluble by autoclaving to induce β-sheet formation. Silk was combined with collagen I to enable PHH attachment using three different methods. First, insoluble (autoclaved) silk scaffolds generated as above were incubated with a 1 mg mL$^{-1}$ collagen I in 1× PBS solution for 2 hours at 37 °C to enable passive collagen I adsorption onto the scaffolds (herein referred to as 'silk + incubated collagen'). Second, lyophilized silk was autoclaved directly in a 1 mg mL$^{-1}$ collagen I in 1× PBS solution (herein referred to as 'silk + autoclaved collagen'). Third, 1 mg mL$^{-1}$ collagen I in 1× PBS solution was added to the silk fibroin solution 3% (w/v) before
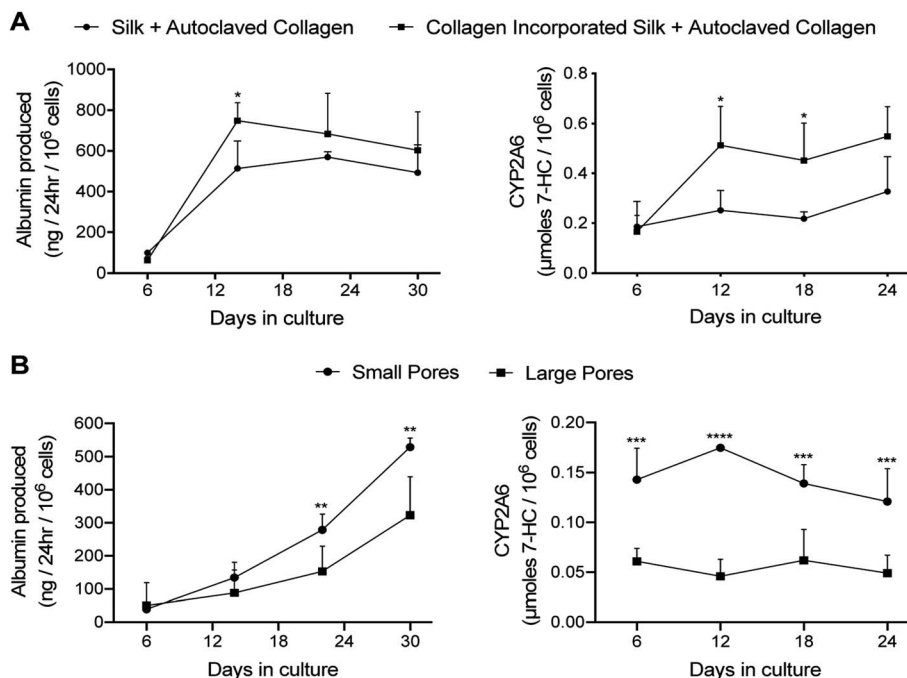
Fig. 3 PHH functions within silk/collagen scaffolds of different pore sizes. Collagen I was incorporated into silk scaffolds by either autoclaving lyophilized silk with a 1 mg mL$^{-1}$ collagen in PBS solution ('Silk + Autoclaved Collagen') or by mixing the solubilized silk solution with 1 mg mL$^{-1}$ collagen in PBS followed by lyophilization and then further autoclaving in 1 mg mL$^{-1}$ collagen in PBS ('collagen incorporated silk + autoclaved collagen'). PHHs were seeded into the scaffolds as described in methods. (A) PHH albumin production and CYP2A6 enzyme activity over time in the two types of silk/collagen scaffolds with small pores (73 ± 25 μm). (B) PHH albumin production and CYP2A6 activity over time in 'collagen incorporated silk + autoclaved collagen' scaffolds with either small or large pores (235 ± 84 μm). *$p \leq 0.05$, **$p \leq 0.01$, ***$p \leq 0.001$, and ****$p \leq 0.0001$.
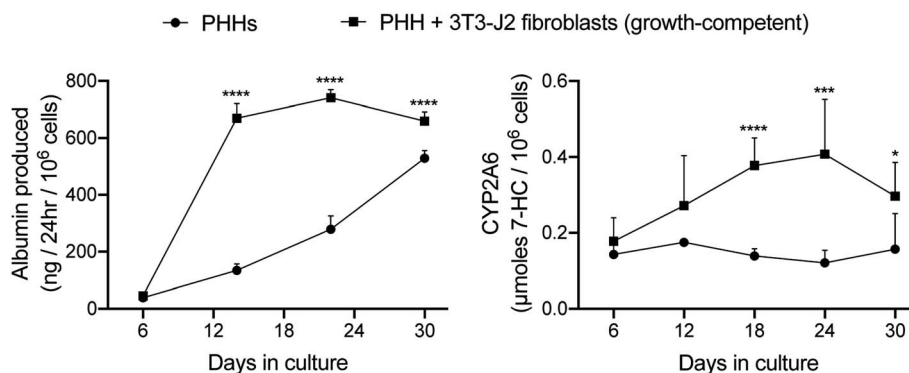


Fig. 4 Functions of PHH-only and PHH + 3T3-J2 fibroblast co-cultures within silk/collagen scaffolds. 'Collagen incorporated silk + autoclaved collagen' scaffolds with small pores (73 ± 25 μm) were fabricated as described in methods. A suspension of either PHH alone (500k cells per scaffold) or PHH + growth-competent 3T3-J2 fibroblasts (1 : 1 ratio, 500k cells for each type) was seeded into the scaffolds. Albumin production and CYP2A6 enzyme activity over time are shown. *$p \leq 0.05$, ***$p \leq 0.001$, and ****$p \leq 0.0001$.

its freezing and lyophilization; then, the silk scaffold containing incorporated collagen was further autoclaved in a 1 mg mL$^{-1}$ collagen I in 1× PBS solution (herein referred to as 'collagen incorporated silk + autoclaved collagen'). After fabrication, silk scaffolds were partially dehydrated by manually squeezing out the hepatocyte culture medium and the PHH suspension was added to the constructs (Fig. 1). Thereafter, PHH attachment and function were assessed in the various porous silk/collagen scaffolds.

The 'silk + incubated collagen' did not yield adequate PHH attachment nor function (data not shown) and thus was not used for further studies. When PHHs were seeded onto 'silk + autoclaved collagen' or 'collagen incorporated silk + autoclaved collagen' scaffolds, sufficient levels of PHH attachment were observed. To visualize PHH attachment in the scaffolds, the scaffolds were fixed, embedded in paraffin, and sectioned for staining over 1, 3, and 5 weeks of culture. PHHs within silk scaffolds stained positively for albumin (Fig. 2 and ESI Fig. 1†)
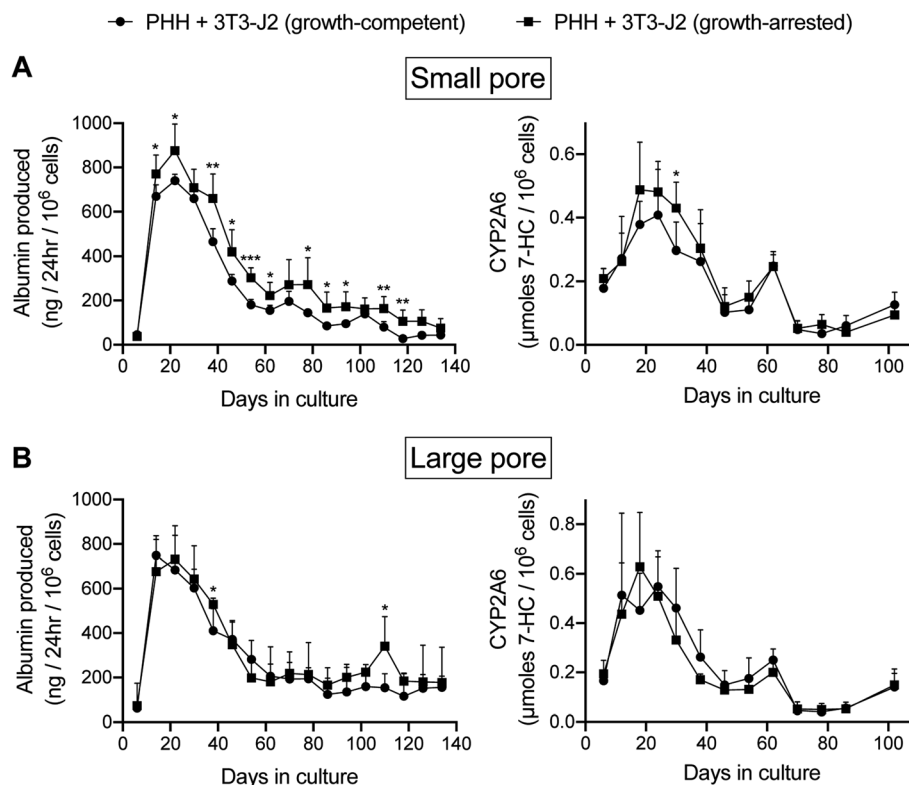
**Fig. 5** Functions of PHHs co-cultured with either growth-competent or growth-arrested 3T3-J2 fibroblasts in silk/collagen scaffolds of different pore sizes. 'Collagen incorporated silk + autoclaved collagen' scaffolds with either (A) small (73 ± 25 μm) or (B) large (235 ± 84 μm) pores were fabricated as described in methods. Albumin production and CYP2A6 activity are shown for the different culture models. *$p \leq 0.05$, **$p \leq 0.01$, and ***$p \leq 0.001$.

and CYP3A4 enzyme (ESI Fig. 2†). While PHHs were found throughout the scaffolds, more cells were found closer to the exterior of the scaffolds with the small pores (∼73 μm ± standard deviation of 25 μm) as can be expected for a passive delivery of cells to a porous scaffold. On the other, PHHs were more homogeneously distributed in the scaffolds with the large pores (∼235 μm ± standard deviation of 84 μm). However, regardless of the pore size, PHHs remained stably housed within the 'silk + autoclaved collagen' or 'collagen incorporated silk + autoclaved collagen' scaffolds for several weeks.

At a functional level, PHHs within 'collagen incorporated silk + autoclaved collagen' scaffolds had ∼1.2- to 1.5-fold higher albumin production and ∼1.7- to 2.3-fold higher CYP2A6 enzyme activity than the 'silk + autoclaved collagen' scaffolds for ∼1 month in culture (Fig. 3A). Therefore, due to the consistent upregulation of PHH function over several weeks in 'collagen incorporated silk + autoclaved collagen' scaffolds, we selected this type of scaffold for all subsequent studies. With respect to the pore size, PHHs within 'collagen incorporated silk + autoclaved collagen' scaffolds with small pores displayed ∼1.5 to 1.8-fold higher albumin production and ∼2.2 to 3.8-fold higher CYP2A6 enzyme activity than the corresponding scaffolds with large pores for ∼1 month in culture (Fig. 3B). Hepatocyte aggregates in small pore and large pore silk scaffolds were found to be ∼43 μm (±standard deviation of 9 μm) and ∼28 μm (±standard deviation of 7 μm) in diameter,

respectively. While larger aggregates were able to form in the smaller pore size, mostly single cell attachment to the silk was observed in the large pore silk scaffolds. Finally, PHHs displayed ∼4- to 4.8-fold higher albumin production in 3D 'collagen incorporated silk + autoclaved collagen' scaffolds (small pore size) than when cultured as conventional monolayers on collagen-coated tissue culture plastic (2D control); additionally, CYP2A6 activity in PHHs was detected only in the 3D silk scaffolds and not in the conventional 2D control (ESI Fig. 3A†).

### Co-culture with NPCs enhances PHH functions within silk/collagen scaffolds

3T3-J2 murine embryonic fibroblasts have been shown to induce functions in PHHs in both 2D and 3D (PEGDA–RGDS) culture formats.[12,34] Therefore, here we sought to determine if a similar outcome could be achieved within the optimized porous silk/collagen scaffolds. The fibroblasts and PHHs were seeded at a 1 : 1 ratio into the 'collagen incorporated silk + autoclaved collagen' scaffolds (small pore size). In such co-cultures, PHHs remained within the scaffolds for at least 5 weeks and stained positive for both albumin (ESI Fig. 1†) and CYP3A4 (ESI Fig. 2†). The presence of the fibroblasts within the scaffolds enhanced PHH albumin production by ∼1.2 to 5-fold
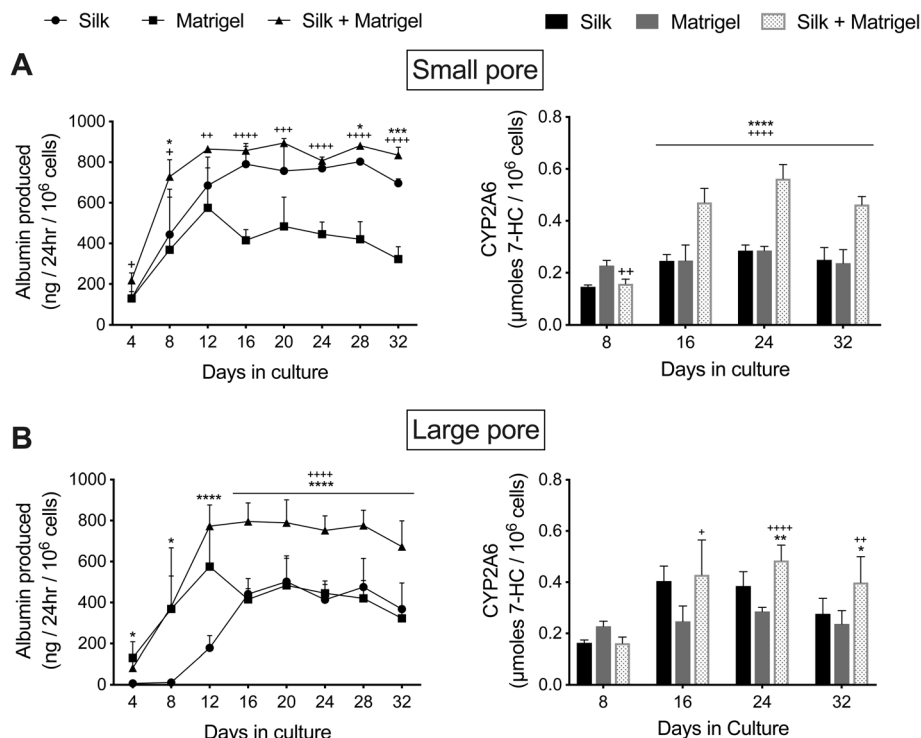
Fig. 6 Functions of PHH/fibroblast co-cultures in silk/collagen scaffolds, polymerized Matrigel only, and silk/collagen that contained polymerized Matrigel. 'Collagen incorporated silk + autoclaved collagen' scaffolds with (A) small ($73 \pm 25$ μm) pores or (B) large ($235 \pm 84$ μm) pores were fabricated as described in methods. The PHH + 3T3-J2 (growth-arrested, 1 : 1 ratio) co-cultures were either suspended in culture medium or a 4 mg mL$^{-1}$ solution of cold Matrigel (growth factor reduced). Next, the co-cultures in culture medium or in Matrigel were dispensed into the silk scaffolds as described in methods and referred to as 'Silk' and 'Silk + Matrigel' conditions, respectively. Additionally, PHHs in Matrigel was dispensed directly into the wells of a 48-well plate as a control condition ('Matrigel'). Upon incubation at 37 °C, the Matrigel polymerized, thereby encapsulating the co-cultures. Albumin production and CYP2A6 activity are shown over time for the different culture models. $*p \leq 0.05$, $**p \leq 0.01$, $***p \leq 0.001$, and $****p \leq 0.0001$ for 'Silk + Matrigel' vs. 'Silk'. $^{+}p \leq 0.05$, $^{++}p \leq 0.01$, $^{+++}p \leq 0.001$, and $^{++++}p \leq 0.0001$ for 'Silk + Matrigel' vs. 'Matrigel'.

and CYP2A6 enzyme activity by ~1.6 to 3.4-fold over ~1 month of culture (Fig. 4).

Due to potential concerns over fibroblast overgrowth within silk scaffolds, the fibroblasts were growth-arrested *via* a pre-incubation with mitomycin-C before mixing with PHHs and seeding into the 'collagen incorporated silk + autoclaved collagen' scaffolds of either small or large pore sizes; PHH function was then tracked for a few months in these co-cultures containing the growth-arrested fibroblasts while using the co-cultures containing the growth-competent fibroblasts as controls. As the growth-competent fibroblasts, the growth-arrested fibroblasts induced both albumin production and CYP2A6 activity in PHHs within both small (Fig. 5A) and large (Fig. 5B) pore scaffolds. While functions in both types of co-cultures were statistically similar within the large pore scaffolds, the growth-arrested fibroblasts induced ~1.4 to 3.8-fold higher PHH albumin secretion in the small pore scaffolds after the first month of culture, whereas CYP2A6 activity was generally similar in both types of co-cultures across both types of pore sizes (Fig. 5B). Furthermore, both growth-competent and growth-arrested fibroblasts induced PHH functions maximally over ~1 month of culture in both small pore or large pore size scaffolds and then the function declined over the next 15–30

days to 20–25% of the maximal levels, following which it declined more slowly over the remaining 2–3 months of culture. Interestingly, co-cultures with both growth-competent and growth-arrested fibroblasts displayed more stable and higher (~1.4- to 2.3-fold) albumin production in the large pore scaffolds in the fourth and fifth months of culture as compared to the small pore scaffolds; in contrast, CYP2A6 activity was similar in both types of co-cultures across both pore sizes for the entire duration of the culture time-period.

In contrast to co-cultures, PHH monocultures within the silk/collagen scaffolds displayed significantly lower (up to 5-fold lower for albumin and up to 10-fold lower for CYP2A6) levels of functions (ESI Fig. 4†) than the PHH/fibroblast co-cultures (Fig. 5); furthermore, while low levels of albumin were detected in the supernatants for 4 months, no CYP2A6 activity was detected after 2 months in the scaffolds with PHH mono-cultures, which was in contrast to the co-cultures.

When compared to conventional (2D) PHH + 3T3-J2 (growth-arrested) co-cultures on collagen-coated plastic, the co-cultures in the 3D 'collagen incorporated silk + autoclaved collagen' produced lower albumin in the first week of culture; however, albumin production in both models was similar from week 2 to week 6 of culture or ~1.2-fold higher in the 3D scaffolds at

certain time-points (ESI Fig. 3B†). As with albumin, CYP2A6 activity in the 2D co-cultures was higher than the silk scaffolds for the first two weeks in culture; however, CYP2A6 activity in the 3D scaffolds became ~1.3-and 2.1-fold higher between week 3 and 5 in culture than the 2D controls, and activity was only detected in 3D scaffolds and not in the 2D controls by week 6.

### Encapsulating PHH/NPC co-cultures in ECM hydrogels enhances liver functions within silk scaffolds

The functions of PHH monolayers on adsorbed collagen have been shown to be enhanced when the cells are overlaid with gelled Matrigel™.[36] Therefore, here we determined whether encapsulating PHH + 3T3-J2 (growth-arrested) co-cultures within growth factor reduced Matrigel (4 mg mL$^{-1}$) before dispensing into the silk scaffolds would further enhance PHH functions. Co-cultures were suspended in an ice-cold 4 mg mL$^{-1}$ Matrigel (growth factor reduced) solution, which was then dispensed into the partially dehydrated 'collagen incorporated silk + autoclaved collagen' scaffolds of either small or large pore sizes (herein referred to as 'Silk + Matrigel'). Control models included equal volumes of co-cultures/Matrigel suspensions dispensed directly into 48-well plates (referred to as 'Matrigel') or co-cultures suspended in an equal volume of culture medium (no Matrigel) dispensed directly into the above silk/collagen scaffolds (referred to as 'Silk'). Silk scaffolds were hybridized with collagen even in the presence of Matrigel (to which PHHs can attach) to enable comparison to PHHs attached to the silk/collagen control scaffold.

As with the 'Silk' and 'Matrigel' control conditions, PHHs remained within the 'Silk + Matrigel' condition for at least 5 weeks and stained positive for both albumin (ESI Fig. 1†) and CYP3A4 (ESI Fig. 2†). Morphologically, co-cultures contracted the 'Matrigel' control scaffold whereas the conditions with silk in them did not show any appreciable contraction (not shown). At a functional level, co-cultures in the 'Silk' control condition with small pores displayed ~1.2- to 2.2-fold higher albumin production and similar CYP2A6 enzyme activity than the 'Matrigel' control between week 2 and week 5 in culture, respectively (Fig. 6A). Furthermore, co-cultures in the 'Silk + Matrigel' condition with small pores displayed ~1.1- to 1.6-fold and ~1.5- to 2.6-fold higher albumin production for 5 weeks in culture than the 'Silk' and 'Matrigel' control conditions, respectively; similarly, co-cultures in the 'Silk + Matrigel' condition with small pores displayed ~1.9- to 2-fold higher CYP2A6 activity between week 2 and week 5 in culture than the 'Silk' and 'Matrigel' control conditions (Fig. 6A).

Co-cultures in the large pore 'Silk' control initially showed for the first 2 weeks lower albumin production and lower CYP2A6 activity than the 'Matrigel' control; however, between week 3 and week 5, co-cultures in the 'Silk' condition produced relatively similar levels of albumin and displayed ~1.2- to 1.6-fold higher CYP2A6 activity than the 'Matrigel' control (Fig. 6B). Furthermore, co-cultures in the 'Silk + Matrigel' condition with large pores displayed ~1.6- to 4.3-fold and ~1.3- to 2.1-fold higher albumin production between week 2 and week 5 in culture than the 'Silk' and 'Matrigel' control conditions,

respectively; similarly, co-cultures in the 'Silk + Matrigel' condition with large pores displayed ~1.1- to 1.4-fold and ~1.7-fold higher CYP2A6 activity between week 2 and week 5 in culture than the 'Silk' and 'Matrigel' control conditions, respectively (Fig. 6B).

Finally, when a type I collagen gel (4 mg mL$^{-1}$) was used instead of Matrigel to embed PHH + 3T3-J2 (growth-arrested) co-cultures before dispensing into the 'collagen incorporated silk + autoclaved collagen' scaffolds (small pores), unlike the 'Matrigel' control, the 'Collagen' control was not contracted to any appreciable degree, which was similar to the 'Silk' control and 'Silk + Collagen' condition (not shown). At a functional level, co-cultures in the 'Collagen' control displayed statistically similar albumin production and CYP2A6 activity as the 'Silk' condition and 'Silk + Collagen' condition over 4–5 weeks in culture (ESI Fig. 5†).

## Discussion

While some biomaterials have been explored to fabricate implantable human liver tissues towards addressing the critical shortage of donor organs for transplantation, there remains a need to further explore PHH interactions with different biomaterials towards determining optimal conditions for their long-term survival *in vitro* and eventual translation to humans. Scaffolds created using silk proteins have highly desirable properties (*i.e.* biocompatibility, tunable mechanical properties, degradation rates, and low immunogenicity) for fabricating implantable tissues. Here, we show for the first time that porous composite silk/collagen scaffolds can be used to elicit functions in PHHs for at least 1 month *in vitro*, and such functions within the silk scaffolds can be further enhanced in the presence of supportive NPCs and when the co-cultures are first encapsulated in a protein hydrogel before housing within the silk scaffold.

Silk proteins have been molded into a variety of shapes, such as hydrogels, tubes, films, and sponges.[37] Here, we selected porous silk (fibroin) sponges[24] since they allow culture medium to penetrate the interior of the scaffolds to maintain cell viability even without perfusion. Furthermore, since silk proteins do not support rapid cell attachment, we combined the silk with rat tail type I collagen (herein referred to as 'collagen I'), which is widely used to enable PHH attachment to various substrates due to its availability in large quantities and cost-effectiveness relative to human-derived proteins.[36] Collagen from different species is well tolerated *in vivo*[38]; however, it has weak mechanical properties and is rapidly degraded post-implantation, so alone, collagen I gels or sponges make poor implant materials.[39] Therefore, combining collagen I with mechanically robust silk that can be tuned for degradation rates is a proven strategy.[20]

Collagen I was incorporated into the silk scaffolds using three different methods. First, insoluble scaffolds were incubated with a solution of collagen I, similar to the strategy used for tissue culture plastic;[36] however, PHHs did not attach well, suggesting that collagen did not adsorb at adequate levels onto the silk scaffolds. In contrast, collagen I incorporated into the

silk during its β-sheet (crystal) formation induced by autoclaving led to robust PHH attachment for several weeks as verified by immunostaining for PHH markers, albumin and CYP3A4; such an effect may be due to integration of the collagen I into the β-sheets. While heat treating collagen is known to denature the native structure of the protein, the necessary cell adhesion components remain intact, allowing for the attachment of hepatocytes to different substrates.[40,41] Further adding collagen during the lyophilization of the solubilized silk solution and then also autoclaving in the collagen I solution similarly promoted PHH attachment. While PHHs attached within silk/collagen scaffolds with both small ($73 \pm 25$ μm) and large ($235 \pm 84$ μm) pores, the distribution of cell attachment was more uniform in the latter though both pore sizes retained PHHs for several weeks as verified by immunostaining.

To appraise PHH functionality, we measured albumin production, a marker of the liver synthetic capability, and CYP2A6 enzyme activity as a marker of the liver drug metabolism capacity. While CYP3A4 is the most abundant CYP450 enzyme in the liver, we were unable to utilize a well-established luminescent assay[34] to assess this enzyme due to a lack of assay performance, which may be due to the binding of the luminescent substrate to the silk proteins; however, PHHs stained for CYP3A4 protein for several weeks in the silk/collagen scaffolds. In contrast, the conversion of coumarin by CYP2A6 into 7-hydroxycoumarin could be readily assessed within silk scaffolds, which tracks similarly to CYP3A4 activity in PHH cultures as we have shown previously.[34] Overall, PHHs cultured within the optimal 'collagen incorporated silk + autoclaved collagen' scaffolds had up to 2.3-fold higher function than the 'silk + autoclaved collagen' scaffolds, suggesting that the addition of collagen during lyophilization and autoclaving is beneficial for PHHs. The mechanism by which this improves PHHs function is hypothesized to be twofold: first, the addition of collagen I at the time of scaffold formation enables entrapment of the collagen I within the silk nanocrystalline domains. This entrapment affords the ability of the cells to robustly bind and pull tension on the silk/collagen scaffold. Secondly, autoclaving in the collagen I solution increases the amount of collagen I passively absorbed to the surface of the silk/collagen scaffold, which aids in initial attachment and cell retention. However, a limitation in this data set is that it is not clear if the increased functionality is due to better retention of PHHs over time within the optimal scaffolds or higher functions on a per cell basis, which we plan to elucidate in future studies. Nonetheless, PHHs in the optimal silk/collagen scaffolds retained functions for at least 1 month and were used for all subsequent studies.

The silk/collagen scaffolds with small pore sizes induced up to ~4-fold higher function than scaffolds with larger pores. Furthermore, hepatocyte aggregate size was ~1.5-fold larger in small pore silk as compared to in large pore silk where mostly single cell attachment to the silk was observed. Since the promotion of homotypic interactions between hepatocytes has been previously shown to be critical for enhancing PHH phenotype in both 2D (*e.g.* confluent monolayers) and 3D (*e.g.* spheroidal) configurations,[36] we anticipate that a similar mechanism is operational in the aggregate size and consequently functional differences observed here between the small and large pore size silk scaffolds. Finally, CYP2A6 activity was not detectable in 2D monocultures on collagen-coated plastic but was well-retained in the 3D silk/collagen scaffolds for several weeks, which is likely due to the promotion of spheroidal morphology of PHHs with minimal spreading in the 3D silk/collagen scaffolds since hepatocyte spreading has been previously shown to inversely correlate with differentiated functions.[42]

Co-culture with liver- and non-liver-derived stromal cell types can positively regulate the survival and functions of hepatocytes in both the pre- and postnatal livers.[43] Such interactions have been previously replicated *in vitro* by co-culturing primary hepatocytes with various liver- and non-liver-derived stromal cell types, including C3H/10T1/2 mouse embryo cells,[44] 3T3-J2 murine embryonic fibroblasts,[43] and human fibroblasts.[45] The 3T3-J2 fibroblasts, in particular, have been shown to express key liver-like molecules, such as decorin[46] and T-cadherin,[47] which help these fibroblasts induce higher levels of functions in PHHs in 2D co-cultures than primary human dermal fibroblasts (not shown), human liver-derived hepatic stellate cells,[48] liver sinusoidal endothelial cells,[49] and Kupffer cells/macrophages.[50] Additionally, 3T3-J2 fibroblasts have been previously shown to lack detectable liver functions,[46,51] which allows for the appraisal of PHH functions within co-cultures. The positive effects of 3T3-J2 on PHH functions have also been shown in 3D PEGDA–RGDS hydrogels both *in vitro* and *in vivo* upon implantation into rodents.[12] However, it is not clear if PEGDA–RGDS hydrogels can maintain the survival and function of PHH-3T3-J2 co-cultures *in vitro* beyond 1–2 weeks, which may be mitigated by the use of a silk/collagen scaffold that, unlike PEGDA–RGDS, allows cells to modulate their contacts and aggregate size over time and facilitates ECM deposition/remodeling due to the porous structure.

The presence of the 3T3-J2 fibroblasts within the optimal silk/collagen scaffolds enhanced PHH functions up to 5-fold relative to PHH-only controls. However, to mitigate any concerns with fibroblast overgrowth within the silk scaffolds, we also growth-arrested the fibroblasts using mitomycin-C (alkylates DNA) before co-culture with PHHs and showed that such a strategy does not affect the ability of the fibroblasts to induce PHH functions. Importantly, in contrast to PHH-only cultures, the effects of the fibroblasts on PHH functions in the optimal silk/collagen scaffolds lasted 5 months. However, co-culture functions in the scaffolds declined after the first month in culture, which suggests that further improvements are needed to the ECM composition within the scaffold and/or media formulation to maintain steady functional levels. For instance, we have recently shown in separate work using PHH/3T3-J2 monolayers that intermittently starving the co-cultures of serum and hormones for 2 days each week significantly prolongs PHH retention and functions by several weeks *via* activation of starvation pathways in PHHs.[52] We anticipate that similar and other abovementioned strategies may ultimately prove useful to maintain PHH functions at steady-state levels within silk/collagen scaffolds for the entire duration of culture.

When compared to conventional 2D PHH/3T3-J2 co-cultures on collagen-coated tissue culture plastic, co-cultures within the 3D silk/collagen scaffolds displayed lower functions in the first 1–2 weeks of culture; such as an outcome is likely due to the prolonged time it takes for 3D aggregates/spheroids of PHHs to adequately form and make sufficient cell–cell adhesions, as also observed in other spheroid generation platforms.[6] However, once the 3D co-cultures had adequately established within the optimal silk/collagen scaffolds, functions in 3D were up to 2-fold higher than 2D; importantly, CYP2A6 activity was detected only in 3D and not in 2D after 6 weeks in culture.

While PHH/3T3-J2 co-cultures housed within silk/collagen scaffolds displayed high function for at least 1 month in culture, the liver has many other ECM proteins that can modulate hepatic functions;[53] furthermore, hepatic functions are enhanced when cultured on or within soft hydrogels.[36,54] Therefore, here we encapsulated PHH/3T3-J2 co-cultures in Matrigel, an ECM routinely used to modulate PHH functions in different culture formats and known to contain many proteins that are also found in liver.[36,55] The encapsulation was done either inside silk/collagen scaffolds or in plastic control wells. Morphologically, co-cultures within the Matrigel-only condition alone contracted over time and detached from plate surfaces, which is a common problem with cell culture in soft gels. However, when Matrigel was injected into the silk/collagen scaffolds, the construct remained intact in size/shape and PHH functions ramped up faster and were up to 2.6-fold higher than the silk/collagen and Matrigel-only control conditions. In contrast, no synergistic increase in coculture function was observed when collagen I gels were entrapped within the silk/collagen scaffolds, suggesting that collagen I alone is not sufficient to promote the highest PHH functions though the PHHs remained stably entrapped within both types of gels that were placed into the silk scaffolds.

Previous investigations using silk scaffolds using either gelatin or RGD as integrin-binding sites for the culture of human liver cell lines (*i.e.*, HepG2 cell line) or rodent hepatocytes have shown minimal inflammation and no adaptive immune response or fibrosis upon implantation into rodents models.[30,32] While it is difficult to fully extrapolate these studies to our work due to the use of different cell types, these previous studies nonetheless show that implanting liver constructs made of silk/ECM scaffolds has promise as a potential therapy that needs further exploration.

While our study determined for the first time the time-dependent functionality of PHHs within porous silk scaffolds hybridized with ECM proteins in the absence or presence of supportive NPCs, several issues will need to be addressed moving forward before translation to humans. First, the PHH infiltration into the scaffolds will need to be improved to enable a greater cell mass by perfusing the cell suspension into the scaffolds using a bioreactor; silk scaffolds are indeed mechanically robust enough to be subjected to perfusion in a bioreactor.[22,23] Second, while 3T3-J2 fibroblasts serve as an initial supportive NPC type to enhance PHH functions and have been previously used in PEGDA–RGDS-based liver surrogates both *in vitro* and *in vivo*,[12] a human NPC counterpart would be needed for human translation. For instance, we have recently shown in a separate study that primary

human hepatic stellate cells can also support some PHH functions within a 3D collagen gel, albeit to a lower level than 3T3-J2 fibroblasts;[56] nonetheless, the use of hepatic stellate cells should help mitigate the concerns with murine fibroblasts for human translation. Third, animal-derived ECM proteins, while widely used for PHH culture due to cost-effectiveness and robust availability,[36] would need to be replaced with human ECM, preferably that derived from decellularized human livers given the many diverse proteins present in liver ECM; however, issues with donor-to-donor variability and cost of acquisition and processing would need to adequately addressed for routine use of decellularized human liver ECM for fabricating implantable liver surrogates. Fourth, incorporation of liver sinusoidal endothelial cells into specific vascular compartments within the silk scaffolds will be necessary to allow the better integration of scaffold vasculature with the host vasculature; indeed, hollow channels can be created by casting the silk scaffold around a mold made of poly-dimethylsiloxane and Teflon-coated wires as was done for intestinal cultures.[33] Inclusion of mesenchymal stem cells with endothelial cells in the silk scaffolds may allow better formation of stabilized neovessels as was done in liver surrogates created using Matrigel and then implanted into rodents.[57] Fifth, while PHHs are most physiologically relevant and strategies are being developed to harness their tremendous expansion potential as *in vivo* using small molecule modulators of key pathways,[9] their use will still necessitate immune-suppression in eventual recipients. While immune suppression *via* drugs is routinely practiced in organ transplantation, the use of induced pluripotent stem cell (iPSC)-derived human liver cells will allow a nearly infinite source of autogenic cells. However, protocols to improve the differentiation of the iPSC-derived human liver cells, including hepatocyte-like cells, need to be significantly improved to induce adult-like functional levels before these cells can be used for routine cell therapy.[8] Finally, the liver has Kupffer cells and cholangiocytes that would need to be included in the scaffolds in compartmentalized domains alongside PHHs to ensure a fully functioning liver for transplantation. Nonetheless, since PHHs perform the majority of liver functions, starting with their long-term culture within silk/ECM scaffolds is an important first step in the development of a liver tissue surrogate.

## Conclusions

We showed for the first time that PHHs display different types of functions within porous silk/collagen scaffolds for at least 1 month *in vitro* and such functions can be further enhanced in the presence of supportive NPCs. Further encapsulating such co-cultures in ECM hydrogels while housed within the silk scaffolds stabilizes the hydrogel and further enhances PHH functions as compared to silk or ECM gel-only controls. Ultimately, PHH/NPC co-cultures within silk/ECM scaffolds can serve as building blocks for strategies in regenerative medicine.

## Author contributions

D. A. K., W. L. S., D. L. K., and S. R. K. designed experiments; D. A. K. and W. L. S. executed experiments; D. A. K. and W. L. S.

analyzed data. D. A. K., W. L. S., D. L. K., and S. R. K. wrote the manuscript.

## Conflicts of interest

The authors have no potential conflicts of interest to disclose.

## Acknowledgements

## References

1 N. Kaplowitz, Idiosyncratic drug hepatotoxicity, *Nat. Rev. Drug Discovery*, 2005, **4**, 489–499, DOI: 10.1038/nrd1750.

2 G. H. Underhill and S. R. Khetani, Emerging trends in modeling human liver disease in vitro, *APL Bioeng.*, 2019, **3**, 040902, DOI: 10.1063/1.5119090.

3 C. J. Murray and A. D. Lopez, Measuring the global burden of disease, *N. Engl. J. Med.*, 2013, **369**, 448–457, DOI: 10.1056/NEJMra1201534.

4 C. J. Murray, *et al.*, Disability-adjusted life years (DALYs) for 291 diseases and injuries in 21 regions, 1990-2010: a systematic analysis for the Global Burden of Disease Study 2010, *Lancet*, 2012, **380**, 2197–2223, DOI: 10.1016/S0140-6736(12)61689-4.

5 S. N. Bhatia, G. H. Underhill, K. S. Zaret and I. J. Fox, Cell and tissue engineering for liver disease, *Sci. Transl. Med.*, 2014, **6**, 245sr242, DOI: 10.1126/scitranslmed.3005975.

6 G. H. Underhill and S. R. Khetani, Bioengineered Liver Models for Drug Testing and Cell Differentiation Studies, *Cell. Mol. Gastroenterol. Hepatol.*, 2018, **5**, 426–439, DOI: 10.1016/j.jcmgh.2017.11.012.

7 H. H. Gerets, *et al.*, Characterization of primary human hepatocytes, HepG2 cells, and HepaRG cells at the mRNA level and CYP activity in response to inducers and their predictivity for the detection of human hepatotoxins, *Cell Biol. Toxicol.*, 2012, **28**, 69–87, DOI: 10.1007/s10565-011-9208-4.

8 R. E. Schwartz, H. E. Fleming, S. R. Khetani and S. N. Bhatia, Pluripotent stem cell-derived hepatocyte-like cells, *Biotechnol. Adv.*, 2014, **32**, 504–513, DOI: 10.1016/j.biotechadv.2014.01.003.

9 J. Shan, *et al.*, Identification of small molecules for human hepatocyte expansion and iPS differentiation, *Nat. Chem. Biol.*, 2013, **9**, 514–520, DOI: 10.1038/nchembio.1270.

10 K. R. Stevens, *et al.*, In situ expansion of engineered human liver tissue in a mouse model of chronic liver disease, *Sci. Transl. Med.*, 2017, **9**(399), eaah5505, DOI: 10.1126/scitranslmed.aah5505.

11 S. Jitraruch, *et al.*, Alginate microencapsulated hepatocytes optimised for transplantation in acute liver failure, *PLoS One*, 2014, **9**, e113609, DOI: 10.1371/journal.pone.0113609.

12 A. A. Chen, *et al.*, Humanized mice with ectopic artificial liver tissues, *Proc. Natl. Acad. Sci. U. S. A.*, 2011, **108**, 11842–11847, DOI: 10.1073/pnas.1101791108.

13 M. B. Browning and E. Cosgriff-Hernandez, Development of a biostable replacement for PEGDA hydrogels, *Biomacromolecules*, 2012, **13**, 779–786, DOI: 10.1021/bm201707z.

14 M. S. Shoichet, Polymer Scaffolds for Biomaterials Applications, *Macromolecules*, 2010, **43**, 581–591, DOI: 10.1021/ma901530r.

15 X. H. Chu, X. L. Shi, Z. Q. Feng, Z. Z. Gu and Y. T. Ding, Chitosan nanofiber scaffold enhances hepatocyte adhesion and function, *Biotechnol. Lett.*, 2009, **31**, 347–352, DOI: 10.1007/s10529-008-9892-1.

16 R. Grant, D. Hay and A. Callanan, From scaffold to structure: the synthetic production of cell derived extracellular matrix for liver tissue engineering, *Biomed. Phys. Eng. Express.*, 2018, **4**, 065015, DOI: 10.1088/2057-1976/aacbe1.

17 F. Croisier and C. Jerome, Chitosan-based biomaterials for tissue engineering, *Eur. Polym. J.*, 2013, **49**, 780–792, DOI: 10.1016/j.eurpolymj.2012.12.009.

18 L. Meinel, *et al.*, The inflammatory responses to silk films in vitro and in vivo, *Biomaterials*, 2005, **26**, 147–155, DOI: 10.1016/j.biomaterials.2004.02.047.

19 E. Manousiouthakis, *et al.*, Bioengineered in vitro enteric nervous system, *J. Tissue Eng. Regener. Med.*, 2019, **13**, 1712–1723, DOI: 10.1002/term.2926.

20 R. D. Abbott, E. P. Kimmerling, D. M. Cairns and D. L. Kaplan, Silk as a Biomaterial to Support Long-Term Three-Dimensional Tissue Cultures, *ACS Appl. Mater. Interfaces*, 2016, **8**, 21861–21868, DOI: 10.1021/acsami.5b12114.

21 R. D. Abbott, *et al.*, The Use of Silk as a Scaffold for Mature, Sustainable Unilocular Adipose 3D Tissue Engineered Systems, *Adv. Healthcare Mater.*, 2016, **5**, 1667–1677, DOI: 10.1002/adhm.201600211.

22 L. Tozzi, *et al.*, Multi-channel silk sponge mimicking bone marrow vascular niche for platelet production, *Biomaterials*, 2018, **178**, 122–133, DOI: 10.1016/j.biomaterials.2018.06.018.

23 W. L. Stoppel, D. Hu, I. J. Domian, D. L. Kaplan and L. D. Black, Anisotropic silk biomaterials containing cardiac extracellular matrix for cardiac tissue engineering, *Biomed. Mater.*, 2015, **10**, 034105, DOI: 10.1088/1748-6041/10/3/034105.

24 J. Rnjak-Kovacina, *et al.*, Lyophilized Silk Sponges: A Versatile Biomaterial Platform for Soft Tissue Engineering, *ACS Biomater. Sci. Eng.*, 2015, **1**, 260–270, DOI: 10.1021/ab500149p.

25 E. S. Gil, S. H. Park, X. Hu, P. Cebe and D. L. Kaplan, Impact of sterilization on the enzymatic degradation and mechanical properties of silk biomaterials, *Macromol. Biosci.*, 2014, **14**, 257–269, DOI: 10.1002/mabi.201300321.

26 J. Rnjak-Kovacina, T. M. DesRochers, K. A. Burke and D. L. Kaplan, The effect of sterilization on silk fibroin biomaterial properties, *Macromol. Biosci.*, 2015, **15**, 861–874, DOI: 10.1002/mabi.201500013.

27 W. L. Stoppel, *et al.*, in *Comprehensive Biomaterials II*, ed. Paul Ducheyne, Elsevier, 2017, pp. 253–278.

28 J. E. Brown, B. P. Partlow, A. M. Berman, M. D. House and D. L. Kaplan, Injectable silk-based biomaterials for cervical tissue augmentation: an in vitro study, *Am. J. Obstet. Gynecol.*, 2016, **214**, 118–119, DOI: 10.1016/j.ajog.2015.08.046.

29 Z. She, W. Liu and Q. Feng, Self-assembly model, hepatocytes attachment and inflammatory response for silk fibroin/chitosan scaffolds, *Biomed. Mater.*, 2009, **4**, 045014, DOI: 10.1088/1748-6041/4/4/045014.

30 G. Janani, S. K. Nandi and B. B. Mandal, Functional hepatocyte clusters on bioactive blend silk matrices towards generating bioartificial liver constructs, *Acta Biomater.*, 2018, **67**, 167–182, DOI: 10.1016/j.actbio.2017.11.053.

31 G. Wei, *et al.*, Three-dimensional coculture of primary hepatocytes and stellate cells in silk scaffold improves hepatic morphology and functionality in vitro, *J. Biomed. Mater. Res., Part A*, 2018, **106**(8), 2171–2180, DOI: 10.1002/jbm.a.36421.

32 Z. Yang, *et al.*, In vitro and in vivo characterization of silk fibroin/gelatin composite scaffolds for liver tissue engineering, *J. Dig. Dis.*, 2012, **13**, 168–178, DOI: 10.1111/j.1751-2980.2011.00566.x.

33 J. Rnjak-Kovacina, L. S. Wray, J. M. Golinski and D. L. Kaplan, Arrayed Hollow Channels in Silk-based Scaffolds Provide Functional Outcomes for Engineering Critically-sized Tissue Constructs, *Adv. Funct. Mater.*, 2014, **24**, 2188–2196, DOI: 10.1002/adfm.201302901.

34 C. Lin, J. Shi, A. Moore and S. R. Khetani, Prediction of drug clearance and drug-drug interactions in microscale cultures of human hepatocytes, *Drug Metab. Dispos.*, 2016, **44**, 127–136, DOI: 10.1124/dmd.115.066027.

35 J. L. Tan, W. Liu, C. M. Nelson, S. Raghavan and C. S. Chen, Simple approach to micropattern cells on common culture substrates by tuning substrate wettability, *Tissue Eng.*, 2004, **10**, 865–872, DOI: 10.1089/1076327041348365.

36 P. Godoy, *et al.*, Recent advances in 2D and 3D in vitro systems using primary hepatocytes, alternative hepatocyte sources and non-parenchymal liver cells and their use in investigating mechanisms of hepatotoxicity, cell signaling, and ADME, *Arch. Toxicol.*, 2013, **87**, 1315–1530, DOI: 10.1007/s00204-013-1078-5.

37 D. N. Rockwood, *et al.*, Materials fabrication from Bombyx mori silk fibroin, *Nat. Protoc.*, 2011, **6**, 1612–1631, DOI: 10.1038/nprot.2011.379.

38 C. H. Lee, A. Singla and Y. Lee, Biomedical applications of collagen, *Int. J. Pharm.*, 2001, **221**, 1–22, DOI: 10.1016/s0378-5173(01)00691-3.

39 A. E. Thurber, F. G. Omenetto and D. L. Kaplan, In vivo bioresponses to silk proteins, *Biomaterials*, 2015, **71**, 145–157, DOI: 10.1016/j.biomaterials.2015.08.039.

40 S. L. Schor and J. Court, Different mechanisms in the attachment of cells to native and denatured collagen, *J. Cell Sci.*, 1979, **38**, 267–281.

41 K. Rubin, M. Hook, B. Obrink and R. Timpl, Substrate adhesion of rat hepatocytes: mechanism of attachment to collagen substrates, *Cell*, 1981, **24**, 463–470, DOI: 10.1016/0092-8674(81)90337-8.

42 R. Singhvi, *et al.*, Engineering cell shape and function, *Science*, 1994, **264**, 696–698.

43 S. N. Bhatia, U. J. Balis, M. L. Yarmush and M. Toner, Effect of cell-cell interactions in preservation of cellular phenotype: cocultivation of hepatocytes and nonparenchymal cells, *FASEB J.*, 1999, **13**, 1883–1900.

44 R. Langenbach, *et al.*, Maintenance of adult rat hepatocytes on C3H/10T1/2 cells, *Cancer Res.*, 1979, **39**, 3509–3514.

45 G. Michalopoulos, F. Russell and C. Biles, Primary cultures of hepatocytes on human fibroblasts, *In Vitro*, 1979, **15**, 796–806.

46 S. R. Khetani, G. Szulgit, J. A. Del Rio, C. Barlow and S. N. Bhatia, Exploring interactions between rat hepatocytes and nonparenchymal cells using gene expression profiling, *Hepatology*, 2004, **40**, 545–554, DOI: 10.1002/hep.20351.

47 S. R. Khetani, A. A. Chen, B. Ranscht and S. N. Bhatia, T-cadherin modulates hepatocyte functions in vitro, *FASEB J.*, 2008, **22**, 3768–3775, DOI: 10.1096/fj.07-105155.

48 M. D. Davidson, D. A. Kukla and S. R. Khetani, Microengineered cultures containing human hepatic stellate cells and hepatocytes for drug development, *Integr. Biol.*, 2017, **9**, 662–677, DOI: 10.1039/c7ib00027h.

49 B. R. Ware, M. J. Durham, C. P. Monckton and S. R. Khetani, A Cell Culture Platform to Maintain Long-term Phenotype of Primary Human Hepatocytes and Endothelial Cells, *Cell. Mol. Gastroenterol. Hepatol.*, 2018, **5**, 187–207, DOI: 10.1016/j.jcmgh.2017.11.007.

50 T. V. Nguyen, *et al.*, Establishment of a hepatocyte-Kupffer cell coculture model for assessment of proinflammatory cytokine effects on metabolizing enzymes and drug transporters, *Drug Metab. Dispos.*, 2015, **43**, 774–785, DOI: 10.1124/dmd.114.061317.

51 S. R. Khetani and S. N. Bhatia, Microscale culture of human liver cells for drug development, *Nat. Biotechnol.*, 2008, **26**, 120–126, DOI: 10.1038/nbt1361.

52 M. D. Davidson and S. R. Khetani, Intermittent Starvation Extends the Functional Lifetime of Primary Human Hepatocyte Cultures, *Toxicol. Sci.*, 2020, **174**, 266–277, DOI: 10.1093/toxsci/kfaa003.

53 R. McClelland, E. Wauthier, J. Uronis and L. Reid, Gradients in the liver's extracellular matrix chemistry from periportal to pericentral zones: influence on human hepatic progenitors, *Tissue Eng., Part A*, 2008, **14**, 59–70, DOI: 10.1089/ten.a.2007.0058.

54 S. S. Desai, *et al.*, Physiological ranges of matrix rigidity modulate primary mouse hepatocyte function in part through hepatocyte nuclear factor 4 alpha, *Hepatology*, 2016, **64**, 261–275, DOI: 10.1002/hep.28450.

55 C. S. Hughes, L. M. Postovit and G. A. Lajoie, Matrigel: a complex protein mixture required for optimal growth of cell culture, *Proteomics*, 2010, **10**, 1886–1890, DOI: 10.1002/pmic.200900758.

56 D. A. Kukla, A. L. Crampton, D. K. Wood and S. R. Khetani, Microscale Collagen and Fibroblast Interactions Enhance Primary Human Hepatocyte Functions in 3-Dimensional Models, *Gene Expression*, 2020, **20**(1), 1–18, DOI: 10.3727/105221620X15868728381608.

57 T. Takebe, *et al.*, Generation of a vascularized and functional human liver from an iPSC-derived organ bud transplant, *Nat. Protoc.*, 2014, **9**, 396–409, DOI: 10.1038/nprot.2014.020.